



Tubule Nanoclay-Organic Heterostructures for Biomedical Applications

Mingxian Liu,* Rawil Fakhrullin, Andrei Novikov, Abhishek Panchal, and Yuri Lvov*

Natural halloysite nanotubes (HNTs) show unique hollow structure, high aspect ratio and adsorption ability, good biocompatibility, and low toxicity, which allow for various biomedical applications in the diagnosis and treatment of diseases. Here, advances in self-assembly of halloysite for cell capturing and bacterial proliferation, coating on biological surfaces and related drug delivery, bone regeneration, bioscaffolds, and cell labeling are summarized. The *in vivo* toxicity of these clay nanotubes is discussed. Halloysite allows for 10–20% drug loading and can extend the delivery time to 10–100 h. These drug-loaded nanotubes are doped into the polymer scaffolds to release the loaded drugs. The rough surfaces fabricated by self-assembly of the clay nanotubes enhance the interactions with tumor cells, and the cell capture efficacy is significantly improved. Since halloysite has no toxicity toward microorganisms, the bacteria composed within these nanotubes can be explored in oil/water emulsion for petroleum spilling bioremediation. Coating of living cells with halloysite can control the cell growth and is not harmful to their viability. Quantum dots immobilized on halloysite were employed for cell labeling and imaging. The concluding academic results combined with the abundant availability of these natural nanotubes promise halloysite applications in personal healthcare and environmental remediation.

applications, including high aspect ratios empty lumen structure, different chemical groups on outer and inner surfaces, high water dispersion stability, good biocompatibility, and high biosafety.^[1–3] Halloysite, with the formula of $\text{Al}_2\text{Si}_2\text{O}_5(\text{OH})_4 \cdot n\text{H}_2\text{O}$, is mined from deposits in many countries such as China, America, New Zealand, Australia, and Turkey. The length of these nanotubes ranges from 200 nm to 2 μm , and the outer and inner diameters are in the range of 50–70 and 10–20 nm, respectively.^[4–6] The morphology and crystal structure of halloysite are given in Figure 1.

Halloysite and polymer/HNTs composites show potential applications in biomedical areas such as tissue engineering scaffold, drug delivery carrier, wound healing dressing, biosensors, cell imaging, and antibacterial materials. For tissue engineering, these clay nanotubes show a significant reinforcing of polymers fibers, porous sponges, and hydrogels. The addition of halloysite increases

1. Introduction

Naturally occurring halloysite nanotubes (HNTs) represent a promising 1D nanomaterial used in biomedical applications. These clay nanotubes have many advantages for biomaterials

the material–cell interactions, which is attributed to the increased surface roughness and the introduction of the bioactive component of the silicon element. The physical properties of composite scaffolds can also be tailored by changing the ratio of polymer and halloysite. For drug delivery, these clay nanotubes can be loaded with chemical drugs, genes, proteins, antibacterial agents, and others. Clay nanotubes have a retardant effect to control the release of these compounds, and can also protect the drugs and promote the drug uptake by cells.^[7,8] The HNTs–drug complex decreases the side effect of drugs due to the lowered drug amount and targeting effect by surface modification. Halloysite has a strong ability to stop bleeding and absorb excess exudates, which leads to the facilitation of cell attachment and promote the healing of the wounds. Chitosan–HNT composite sponges and poly(L-lactide)/HNTs electrospun mats can be used in skin wound healing materials. These attribute to the proper porosity, enhanced mechanical properties, enhanced blood clotting, and good biocompatibility by the incorporation of the nanotubes.^[9,10] For biosensor application, the integration of enzymes onto halloysite surfaces can improve the direct electron transfer between immobilized enzymes and electrode surface for highly sensitive enzymatic biosensors.^[11] Incorporation of metallic nanoparticles on the clay nanotubes enhanced amperometric glucose sensing performance by

Prof. M. Liu, Dr. R. Fakhrullin, Dr. A. Panchal, Prof. Y. Lvov
Institute for Micromanufacturing
Louisiana Tech University
Ruston, LA 71270, USA
E-mail: liumx@latech.edu; ylvov@latech.edu

Prof. M. Liu
Department of Materials Science and Engineering
Jinan University
Guangzhou 510632, P. R. China

Dr. R. Fakhrullin
Bionanotechnology Lab
Kazan Federal University
Kazan 420008, Republic of Tatarstan, Russian Federation

Dr. A. Novikov, Prof. Y. Lvov
Functional Aluminosilicate Nanomaterials Lab
Gubkin Russian State University of Oil and Gas
Moscow 119991, Russia

The ORCID identification number(s) for the author(s) of this article can be found under <https://doi.org/10.1002/mabi.201800419>.

DOI: 10.1002/mabi.201800419

metal nanoparticle-mediated conductivity. Coating halloysite on plastic microtubes or their self-assembled pattern can be used to capture circulating tumor cells (CTCs) from blood samples, which can be designed as a biosensor for an early diagnosis of cancer.^[12] Conjugation of antibodies such as anti-EpCAM on the nanoclay surfaces can enhance the capture efficacy and purity. Halloysite can also be loaded with different inorganic and organic compounds for antibacterial materials. For example, halloysite-supported silver and ZnO nanoparticles showed synergistically enhanced antibacterial activity toward *Escherichia coli*.^[13] The typical application of the clay nanotubes in biomedical areas is presented in **Figure 2**.

We discuss recent halloysite research emphasizing our vision in self-assembly of the clay nanotubes for several different purposes while reviewing the toxicity of halloysite. Self-assembly of these clay nanotubes in functional arrays following the principles of macromolecule self-organization (like nematic liquid crystal orientation) allows for production of organized organic/inorganic structures for biomedicine. These objective goals include cell capture and bacterial proliferation, coating and related drug delivery, bone regeneration, bioscaffold, and cell labeling. All these results suggest that halloysite shows promising applications in different biomedical areas, which also promotes the practical application of this tubule nanoclay in personal healthcare and environmental science.

2. Micropattern Self-Assembly for Cell Capture and Bacterial Proliferation

2.1. Cell Capture

Halloysite can be well dispersed in water with the aid of surfactants,^[12,14] and its stable aqueous dispersion can be utilized to self-assemble into regular patterns. This micropattern can be used as cell growth supporting scaffolds and cell capture devices.^[15] Due to the high aspect ratio of the clay nanotubes, their alignment in the micropatterns can also be controlled by adjusting the conditions such as concentration, drying temperature, evaporation time, and confined spaces. Highly ordered nanotube patterns with droplet-casting evaporation of halloysite dispersion were developed.^[16] These clay nanotubes form a “coffee-ring” deposit and align along the droplet edge when dried. This work provided a first example of self-assembly of the clay nanotubes into a regular pattern, but it cannot be used to prepare large area micropatterns.

Subsequently, glass capillary tubes were used to control evaporation of the nanoclay aqueous dispersion to prepare patterned surface with ordered nanotubes alignment.^[17] Before preparation of halloysite patterned surface, sodium polystyrene sulfonate (PSS) was used to modify halloysite to improve the surface charges of the tubes and increase the dispersion stability. When drying PSS-HNTs aqueous dispersion in glass tubes with diameter of 7 mm, a regular strip-like pattern is formed in the inner wall of the glass tubes. The formation of strip pattern can be understood by the coffee-ring effect. The loss of water at the capillary edges causes the pinning of the solid-liquid-gas three phase contact line (i.e., “stick”), thereby forming the outmost ring. Upon drying, the contact angle of



Mingxian Liu received his B.Sc. (2004) in macromolecular science and engineering from Qingdao University of Science and Technology, and his Ph.D. (2010) from the South China University of Technology. He is now a full professor in Department of Materials Science and Engineering at Jinan University. He visited

the Institute for Micromanufacturing at Louisiana Tech University (USA) for 9 months in 2018–2019. His current research is in the areas of biomaterials, biomedical polymers, controlled release, tissue engineering, and cancer diagnose.



Rawil Fakhruллин is principal investigator at the Institute of Fundamental Medicine and Biology, Kazan Federal University (Republic of Tatarstan, RF), where he received his Ph.D. in 2006. He has worked as a visiting scientist in Universities of Hull and Sheffield (UK), Yeditepe University (Turkey), and Louisiana Tech University

(USA). In 2016, he has been conferred the title of visiting professor by University of Palermo (Sicily, Italy). His research areas are cell-surface engineering, clay-based nanomaterials, and nanotoxicity.



Yuri M. Lvov received Ph.D. from M. Lomonosov Moscow State University in 1979 and then worked at Max Plank Institute for Colloids and Interfaces, Germany, National Institute for Material Sciences, Tsukuba, Japan and Naval Research Laboratory, USA. He is professor of chemistry and T. Pipes Eminent Endowed Chair

on micro and nanosystems at Louisiana Tech University, USA. His area of interests is nanoassembly of organized films, ordered shells on tiny templates, clay nanotubes for controlled release of chemical agents, functional organic-inorganic nanocomposites.

the capillary edge decreases gradually to a critical angle at which the gravity (depinning force) becomes larger than the pinning force. This results in a hop of the contact line to a new position

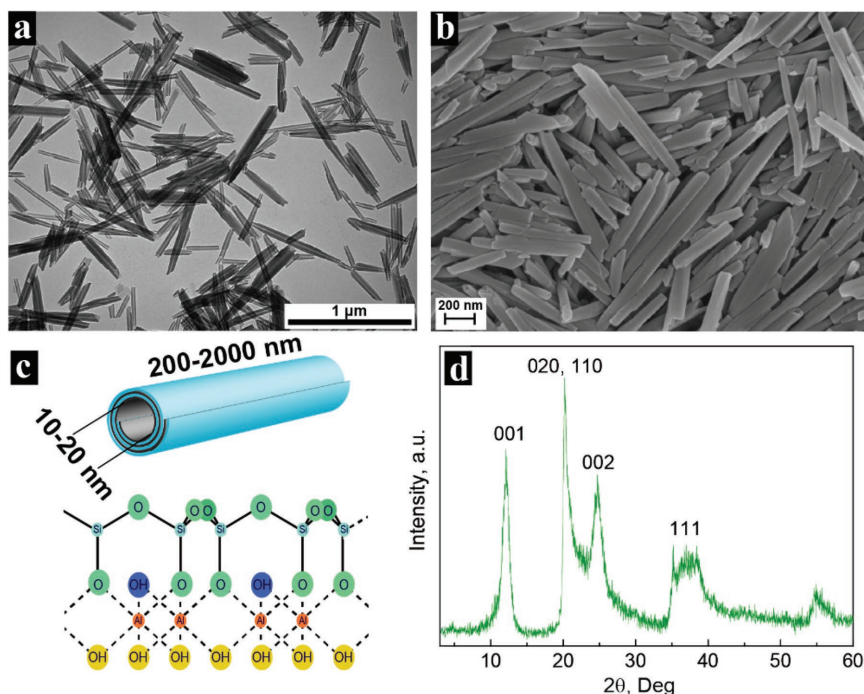


Figure 1. Morphology and crystal structure of halloysite (sample mined from Shanxi, China): a) TEM images; b) SEM images; c) Crystal structure; d) XRD pattern.

(i.e., “slip”), where a new ring deposit is formed. The repetition of the “stick–slip” motion of the contact line causes the formation of halloysite strips on the wall of the glass tube from top to the bottom. The width and spacing of the bands depend on the halloysite dispersion concentration, the drying temperature, and the sizes increase with the concentration and decrease with the drying temperature. **Figure 3** shows the optical images of the formed micropattern from different clay concentrations.

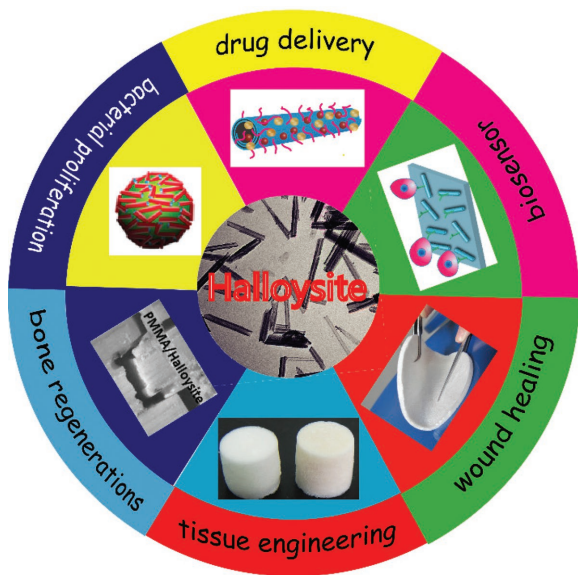


Figure 2. Application of halloysite nanotubes in biomedical areas.

Interestingly, a high degree of alignment of nanotubes in the strips is found at the sample prepared from 10% concentration and the half height peak width of nanotubes angular distribution is only 10.4°. This is related to the formation of liquid crystal phenomena at high nanoclay concentration. The patterned HNT surface can serve as a template for preparing polydimethylsiloxane molding. Moreover, the rough surfaces of halloysite pattern show increased interactions with tumor cells, providing enhanced tumor cell capture efficiency compared to bare glass surfaces. The maximum Neuro-2a cell capture efficiency of 88% is achieved for 3 h culture on the halloysite patterned surfaces.

With a confined space for drying, the PSS-HNTs dispersion and strip-like patterned coating on glass substrate can be obtained after the self-assembly process.^[18] The PSS-HNTs dispersion was injected into a slit which is composed by two glass slides and two gaskets. The dispersion was subsequently dried at 60 °C for 12 h. It is found that regular strips with cracks between them can be formed on the glass slide, and the strips become

regular and almost parallel to each other when the halloysite concentration increases. The maximum nanotube alignment degree can be achieved at 2% PSS-HNTs dispersion. The formed halloysite patterned coating was then employed to capture tumor cells from different liquid media including blood sample. Due to the enhanced interfacial interactions between halloysite and cells, the tumor cell capture efficacy is higher on the nanostructured coatings than that on blank glass surfaces. The capture yield of many typical tumor cells including HepG-2 cell, MCF-7 cell, Neuro-2a cell, A549 cell, and B16F10 cell on the nanotube-coated surface is above 80% in cell culture medium. When anti-EpCAM is conjugated to halloysite, the capture yield of tumor cells can reach 92% after 3 h incubation. Then the capture experiment was preceded in peripheral blood samples. The calculated MCF-7 cells were mixed into healthy human blood at different concentrations of 10, 20, 50, 100, and 200 cells mL⁻¹. The anti-EpCAM conjugated patterned halloysite coatings exhibit ≈80% capture efficiency of targeted MCF-7 cells. Particularly, 2% nanotube coating can capture eight MCF-7 cells from 1 mL artificial blood samples containing ten cells. The preparation method of the nanotube patterned surface is fast, and the cell capture performance is high. Therefore, this system shows promising application in clinical CTC capture for early diagnosis and monitoring of cancer patients. The preparation and tumor cell capture process of patterned halloysite coating are shown in **Figure 4**.

Highly ordered and concentric ring patterns with hierarchical cholesteric architectures can be obtained by evaporation-induced self-assembly of halloysite dispersion in a sphere-on-flat geometry.^[19] It is found that the width of

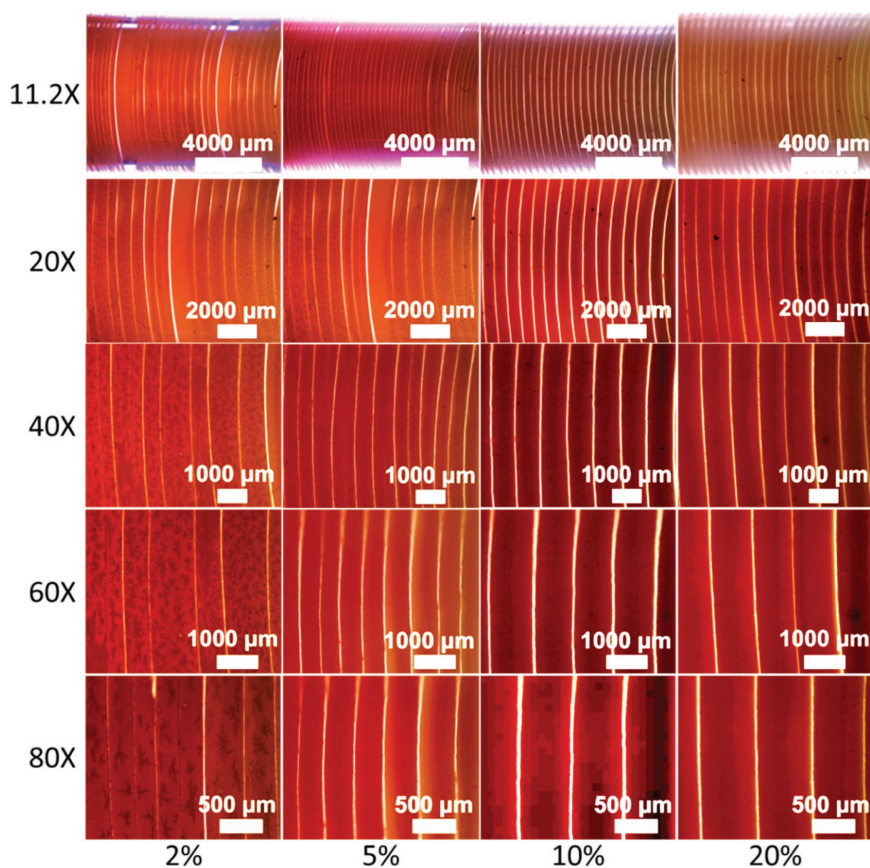


Figure 3. The optical images of the formed halloysite patterns from different concentrations. Reproduced with permission.^[17] Copyright 2016, American Chemical Society.

the inner ring, outer ring, and spacing between the adjacent rings are proportionate to halloysite concentration. Interestingly, the highly ordered and concentric halloysite rings show pronounced Maltese cross-like pattern under crossed polarizers, and this is the first time that HNT patterned surfaces with hierarchical cholesteric architecture are observed. The polarized optical images of halloysite pattern formed by

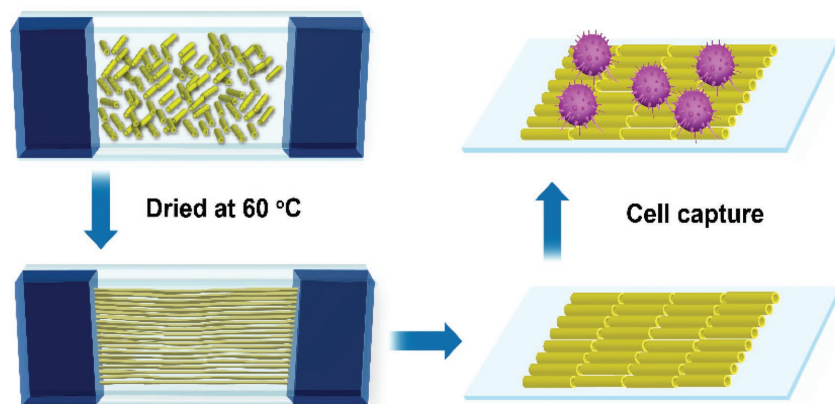


Figure 4. The preparation and tumor cell capture process of patterned HNTs coating in a slit-like confined space. Adapted with permission.^[18] Copyright 2017, Royal Society of Chemistry.

self-assembly in a sphere-on-flat geometry is shown in **Figure 5**. A disclination alignment of the nanotubes in the ring strips with high nanotube suspension concentration can be recognized from morphology observation. The patterned halloysite surfaces were then employed as cell supporting substrates. The rings can guide the growth and orientation of C2C12 myoblasts cells. This work is also a simple, repeatable, mild, and high efficiency method for obtaining halloysite hierarchical architectures. The nanotube patterned surfaces with concentric rings show promising applications in vascular grafts and skin regeneration.

Besides the utilization of the confined spacing for drying halloysite dispersion, rough coatings can be prepared by thermal spraying of the nanoclay ethanol dispersions.^[20] A different thickness halloysite coating with high transparency and tailorable surface roughness can be obtained after evaporation of the solvent (ethanol). The halloysite coatings are also employed to capture cells from artificial blood samples or blood samples from patients with metastatic breast cancer. Similarly, the tumor cells can be captured effectively by halloysite coatings (except HeLa cells), while blank glass surfaces show a very low cell capture yield. The cell capture yield can be changed by altering the HNT ethanol

dispersions concentration, and maximum MCF-7 cell capture yield of 90% can be achieved by anti-EpCAM conjugated 2% halloysite rough coating. Further incorporation of dynamic shear using a peristaltic pump would enable the cells capture yield of halloysite coating, improving it to 93% within 2 h. The schematic showing the capture process of HNT thermally sprayed surfaces under dynamic shearing toward tumor cells is shown in **Figure 6**. Anticancer drug doxorubicin-loaded halloysite can also be sprayed into a uniform coating. The captured MCF-7 cells on drug-loaded nanotube coating exhibit serious membrane rupture morphology and the cell viability is only 3% after 16 h due to release of the drug. The high capture and killing ability of doxorubicin-loaded HNT coating can be designed as an implantable diagnosis and therapeutic device for tumor metastasis.

2.2. Halloysite-Stabilized Oil Microdroplets and Bacterial Proliferation

The spilling of raw petroleum in sea causes both acute and long-term environmental

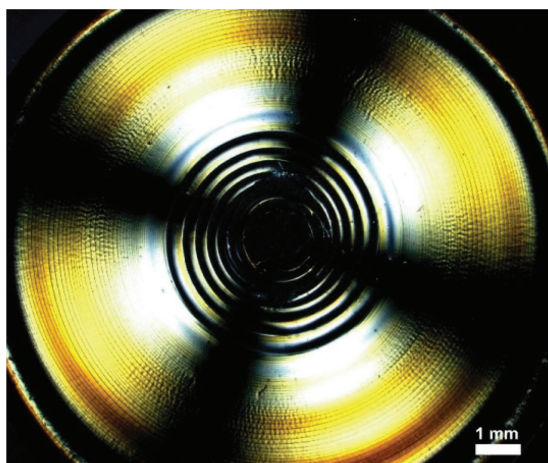


Figure 5. The polarized optical images of halloysite pattern formed by self-assembly in a sphere-on-flat geometry. Reproduced with permission.^[19] Copyright 2016, American Chemical Society.

problems due to its toxicity. Oil-degrading microorganisms can consume and degrade it at a higher efficiency if petroleum is micro-emulsified, though their concentration is rather low. It is important to find an effective carrier for better proliferation of these microorganisms, and it is best if this carrier will also enhance emulsification process. HNTs were introduced as inexpensive natural particles that stabilize petroleum emulsions. Halloysite as an efficient agent for emulsification has been explored keeping in view applications such as oil spill bioremediation^[21–23] and mesocatalysts.^[21,24,25] Oil Pickering emulsification can proceed with

energies low enough to be afforded by ocean turbulence and the stability of droplets extends over more than a week. Elliptical and cylindrical shape of nanoparticles are more effective at stabilizing interfaces compared to spherical particles, so halloysite usage is advantageous.^[26] Surface modification, such as grafting silane molecules and carbonizing chitosan, is effective at converting the hydrophilic external of the nanotubes to hydrophobic surface.^[21,26,27] The oil/water interface is shown to be roughened with nanoclay and bacteria, providing oil degradation, are better attached to such oil droplets than to droplets without halloysite (**Figure 7**). The metabolic activity of *Alcanivorax borkumensis*, an alkanotrophic bacteria widely distributed in marine environments (particularly in Mexican Gulf), is enhanced by halloysite addition. A HNTs-based dispersant system is therefore environmentally friendly and promising for further scale-up optimization. The key elements of the described formulations are natural clay nanotubes and are abundantly available in thousands of tons, thus making this technology scalable for environmental petroleum spill bioremediation.

3. Microfiber Halloysite Coating with Dye/Drug Delivery

As an extension of the self-assembly approach, we also performed halloysite coating on hair surface. Hair is a proteinaceous construct of the human body with 65–95% keratin, lipids, water, and pigments making up the rest.^[28] Structurally, hair is majorly divided into a cortex, which is the core fiber and the outer covering called cuticle.^[29] Researchers have used the plate-like cuticle covering to

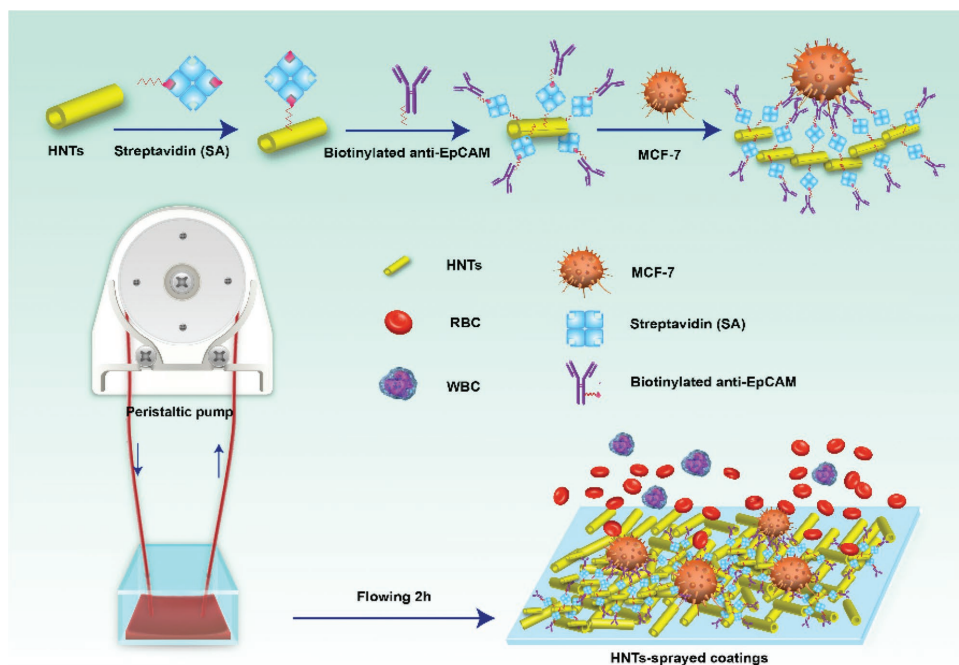


Figure 6. Schematic diagram showing the modification of halloysite and the cell capture process from whole blood using a circulating device with a peristaltic pump. Reproduced with permission.^[20] Copyright 2018, Elsevier.

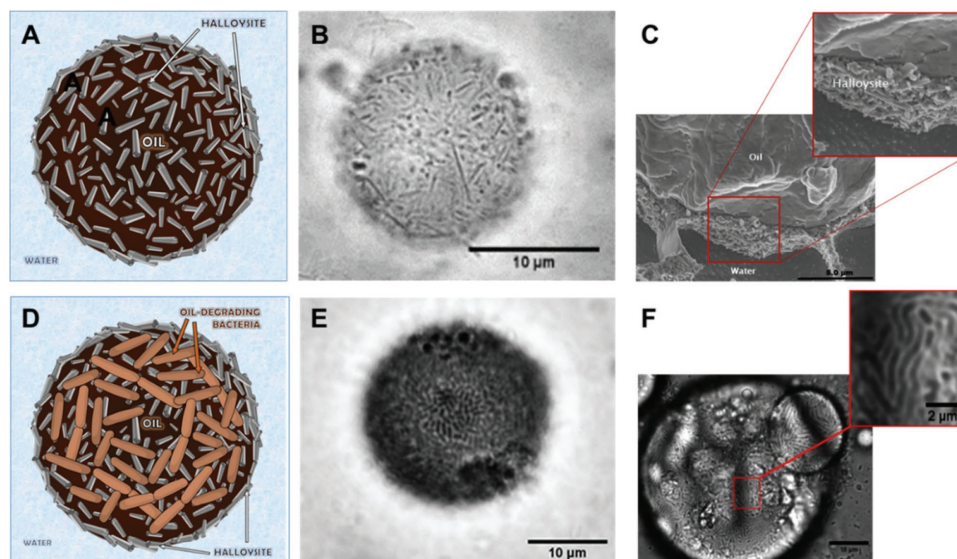


Figure 7. a–c) Scheme of halloysite Pickering emulsion followed by optical microscope image and cryo-SEM image of one emulsion droplet indicating clay nanotubes at the oil–water interface (inset). d–f) Halloysite Pickering emulsion for oil spill bioremediation covered with oil-degrading bacteria followed by optical microscope images of emulsion droplets dotted with rod-shaped *Alcanivorax borkumensis* bacteria. b) Reproduced with permission.^[27] Copyright 2017, Wiley-VCH. a, c–f) Reproduced with permission.^[27] Copyright 2018, Elsevier.

design self-assembly–based haircare formulations.^[30] Out of the $\approx 30\ \mu\text{m}$ diameter of hair, cuticles are only $1\ \mu\text{m}$ thick and each plate is $5\text{--}10\ \mu\text{m}$ long. These plates are attached to one another by the root end leaving their tail end overlapping with the preceding one. The cuticles swell when wetted with any aqueous solvent, creating cavities around the roots of each cuticle when they open up.^[31] Halloysite dispersion enters the newly formed cavities and upon the loss of water, start getting pushed into the narrow cavity due to capillary forces. The phenomenon of the HNTs accumulating beneath the cuticles can be governed by the Marangoni flow forces (or the “coffee-ring” effect).^[16,19] The deposit of the nanotubes from the root ends while drying continues over the remaining part toward the tail end and almost all the hair is coated with halloysite (Figure 8).

Halloysite covers the hair surface in a $1\text{--}3\ \mu\text{m}$ thick layer and the coating is quite robust, lasting up to ten shampoo washes. With their inherent ability to load molecules inside the lumen and release them in a sustained and controlled manner,^[1,32,33] surface engineering of hair with halloysite creates a novel approach to deliver active chemicals to the surface of hair. The delivery can be applicable to both water-soluble and water-insoluble compounds; however, for water-insoluble compounds, raw halloysite must undergo surface modifications to be able load them inside the lumen. The halloysite lumen lined

with positively charged alumina groups is polar and hydrophilic. Hydrophilic compounds are pulled into the cavity and retained there until release. The loading of hydrophobic dyes, drugs, grafting octadecylphosphonic acid via covalent linkages, and physisorption of negatively charged long alkyl surfactant molecules has been done.^[34,35] The inclusion of molecules on both sides of the hydrophobicity–hydrophilicity spectrum into the hair drug delivery approach makes multiple formulations possible. Hair color with natural dyes is

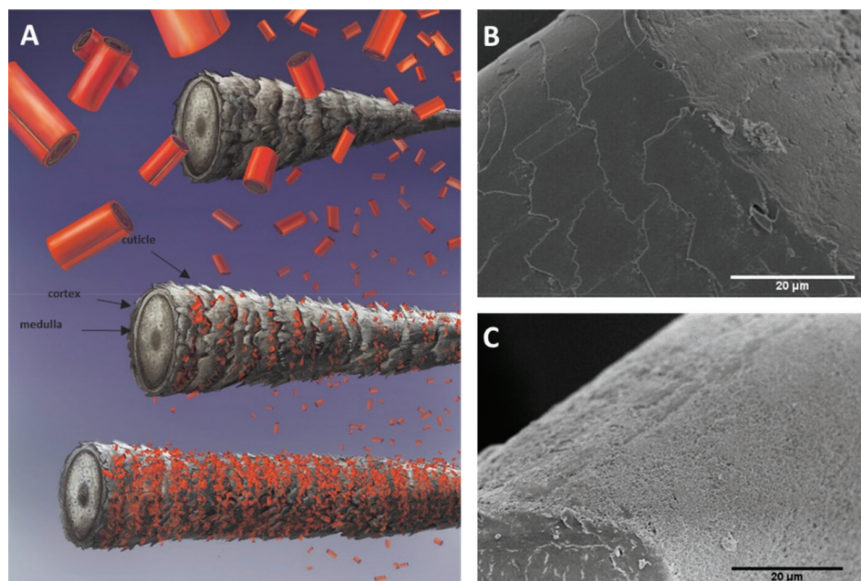


Figure 8. Illustration of the assembly process of the nanotubes from their dispersion onto hair. (A) Bare (B) and coated (C) cuticle surface of hair. Reproduced with permission.^[30] Copyright 2018, Royal Society of Chemistry.

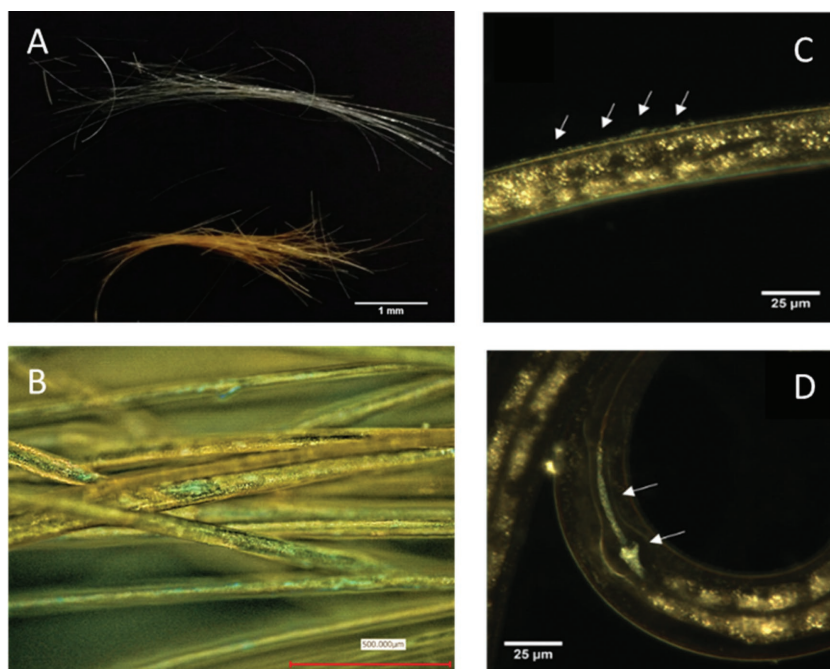


Figure 9. a) Grey human hair before (top) and after (bottom) coating with lawsone-loaded clay nanotubes. b) High definition collated image of colored hair. The presence of halloysite on the surface is visible. c,d) Dark-field microscopy images of *Caenorhabditis elegans* undergoing exposure to permethrin-loaded nanotubes. The white arrows point to halloysite on surface (c) and inside the intestines of the microworm (d). Reproduced with permission.^[30] Copyright 2018, Royal Society of Chemistry.

an evident and eye-catching application with the researchers successfully dyeing human grey hair by the natural henna dye in under 5 min from nothing but an aqueous dispersion of lawsone-loaded halloysite, dilute acetic acid, and water^[30,36] (Figure 9). A significant possibility is the development of anti-lice formulations. Most of the anti-lice drugs are highly water insoluble and toxic with the additional problem of resistance development by repeated treatments.^[37–39] With the directed delivery of water-insoluble compounds like permethrin to the site of lice infestation—cuticle, the authors have proposed to reduce the dosage and chances of lice to develop resistance.^[30]

Insecticides which have a similar chemical nature can be developed for veterinary formulations as the hair assembly is shown to work on hairs from species like dog, cat, and horse.^[30] The specific release to the site also increases the efficacy of the insecticide inside the lumen. More applications that are viable using this technique of loading and release on hair surface such as hair loss control, hair thickening, hair strengthening, and topical cosmetics. Since many other natural fibers possess a similar external surface as hair, the ubiquitous self-assembly works equally well on natural silk and wool fibers.

Physical–chemical properties of the tubule clay allow for drug loading, sustained release with extended control of duration through the end tube capping with polymers. Development of HNTs-polymer composites such as tissue scaffolds and bone cement/dentist resin formulations with enhanced mechanical properties and extension of the drug release to 2–3 weeks has been described.^[40] Various drugs were loaded at 5–15 wt% into halloysite and allowed for extended release during 10–20 h; as examples, we may mention: khellin, oxytetracycline, gentamicin, ciprofloxacin, vancomycin, atorvastatin, metronidazole, dexamethasone, doxorubicin, furosemide, nifedipine, curcumin, resveratrol, and antiseptics—povidone iodine, amoxicillin, brilliant green, chlorhexidine, DNA, and viral genes.^[40–42] Biocomposite films based on pectin and halloysite loaded with salicylic acid also showed an extended antimicrobial activity.^[43]

The typical release profiles of the drugs loaded in the clay nanotubes as compared to release of the drug microcrystals are presented in Figure 10. The drug release from this clay was much longer than that from the microcrystals. For nifedipine, it was 25 times longer, and in the case of furosemide and dexamethasone it was 75 times longer. In all three release curves, there is

an initial burst within 10 min followed by a 6–10 h extended release.

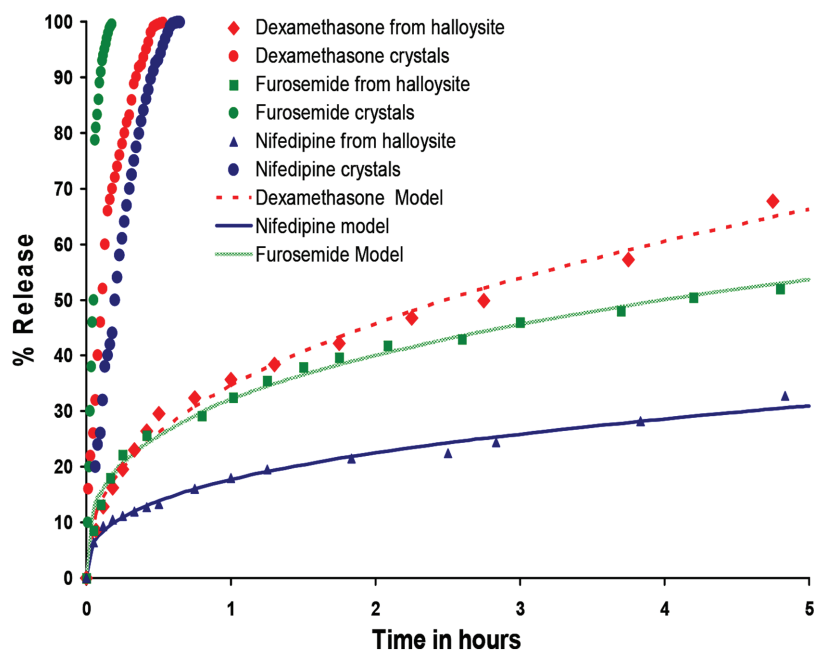


Figure 10. Release profiles of the drugs from halloysite in water at pH 7.4: loading from 10% alcohol/water.^[1]



4. Bone Regeneration, Bioscaffold, Cell Coating, and Labeling

4.1. Bone Regeneration

Bone cement is used in surgery for effectively filling cavities, and to create a mechanical fixation; it is composed of synthetic and self-curing organic or inorganic material. Poly(methyl methacrylate) (PMMA) has been successfully used in clinical applications for several decades, because of its excellent tissue compatibility and good processability. However, there is a critical trend to enhance its structural integrity and to control antibiotic release (antibiotics cannot survive the curing process if they are directly added to the mixture before polymerization). Halloysite was loaded with antibiotic—gentamicin sulfate, and then the PMMA composite cement was formulated with 7 wt% drug-loaded nanotubes.^[44] This formulation protected the drug from methyl methacrylate acting as containers for the antibiotic. By incorporation of halloysite into PMMA, the antibiotic release was ≈ 3 weeks after applications. The release of antibiotics from this composite effectively inhibited *E. coli* and *S. Aureus* bacterial growth. Moreover, the tensile strength and adhesion to bone of the composite was significantly increased. Recently, 3D printing drug-doped halloysite with polylactic acid was used to fabricate antimicrobial devices for bone regeneration.^[45] The loaded gentamicin was released in a sustained manner from these systems and exhibited an excellent antibacterial inhibition.

4.2. Bioscaffold

Tissue engineering scaffolds are generally made with artificial or natural polymers to support cell growth. The common requirements for these scaffolds are porous, cyto- and tissue compatible, bioactive, and mechanically strong. Halloysite has been incorporated into biodegradable polymers to prepare tissue engineering scaffolds. Polyvinyl alcohol/HNTs bio-nanocomposite films can support the growth of osteoblast and fibroblast cells.^[46] The addition of halloysite into chitosan scaffolds also brings a significantly enhanced compressive strength, compressive modulus, and thermal stability.^[47] Meanwhile, the nanotubes had little effect on the pore structure and porosity of the polymer scaffolds. Mouse fibroblasts could develop well on the composite surfaces even at 80 wt% the nanotube content. Electrospun HNTs-PLGA nanofibrous mats also exhibited excellent biocompatibility and controlled drug delivery behavior.^[48] Cell proliferation assay showed that halloysite did not significantly influence the cell viability compared to the pure PLGA fibers. The composite scaffolds could provide a 3D structure with interconnected pores for cell attachment and migration. The fibroblast cells cultured on the nanocomposite scaffolds displayed a phenotypic shape, suggesting that the cells could penetrate and migrate within the scaffolds similar to native extracellular matrix. Therefore, the doping of the clay nanotubes into polymer scaffolds shows great potential for applications in tissue engineering.

4.3. Cell Coating with Halloysite

Most of the published applications of halloysite are either related to biomedical formulations and devices, or imply that the nanotubes might be brought in contact with organisms and environment as a result of unintended exposure.^[1] Therefore, halloysite was subject to numerous toxicity and biocompatibility evaluation studies,^[49] predominantly demonstrating very low toxicity of either pristine^[50] or modified halloysite.^[51] Experiments were carried out using microorganisms, cultured human cells, and in vivo models to meticulously investigate the toxicity of clay nanotubes. These clay nanotubes were found to be not toxic toward microorganisms as demonstrated using yeast^[52] and bacteria.^[53] Yeast cells were incubated with pristine halloysite; in addition, layer-by-layer polyelectrolyte assembly was applied to attach nanotubes to cell walls. Using fluorescein diacetate and propidium iodide fluorescence viability test, the authors have confirmed that around 83% of layer-by-layer HNT-coated cells were viable (Figure 11a), whereas the viability of cells mixed with halloysite was almost the same as in intact cells.^[52] Budding yeast cells were detected using scanning electron microscopy, further confirming the biocompatibility of the nanoclay coatings (Figure 11b). Importantly, halloysite doped with intrinsically nontoxic nanoparticles does not show any synergistic adverse effects of microbial viability, as show for magnetite-doped halloysite using yeast cells and a set of viability and proliferation tests.^[54] Bacteria have also been subjected to halloysite, several studies have shown very low toxicity of pristine clay nanotubes toward *E. coli*^[55] and *A. borkumensis*,^[21] while the other report suggests that halloysite has shown notable toxicity effects on several *Salmonella typhimurium* strains.^[53]

Human cell cultures, as models for intracellular drug delivery, have been extensively subjected to halloysite to investigate the uptake mechanism. Several types of human cells, both cancer cell lines and primary cultures were treated with halloysite at different concentrations, demonstrating an effective uptake (Figure 11c,d) and distribution in cytoplasm.^[56–58] Notably, cells with altered metabolic activity have demonstrated different nanotube uptake rates. This allows for using halloysite as a drug delivery vehicle for intracellular administration of curcumin^[57] and paclitaxel.^[59] Polymer-modified shortened clay nanotubes were successfully employed for gene delivery, indicating the possible nuclear uptake.^[42]

4.4. Halloysite/Quantum Dots for Cell Labeling

HNTs-azine-CdS quantum dot composites were synthesized by reaction between cadmium nitrate and thioacetamide.^[60] HNTs-azine-CdS composite is a yellow powder which is well dispersible in water (Figure 12C). The fluorescence spectra of these nanocomposites cover a broad range up to 630 nm when excited with 405-nm or 457-nm laser. The sharp minima at the fluorescence spectra (at 488 or 514 nm) visible in Figure 12A are attributed to the confocal microscope filter cube. Individual clay nanotube in the sample is covered with CdS particles of 5–10 nm diameter (Figure 12B), that emit fluorescence when excited with laser. The fluorescence of HNTs-azine-CdS composites is observed along with the pronounced scattering

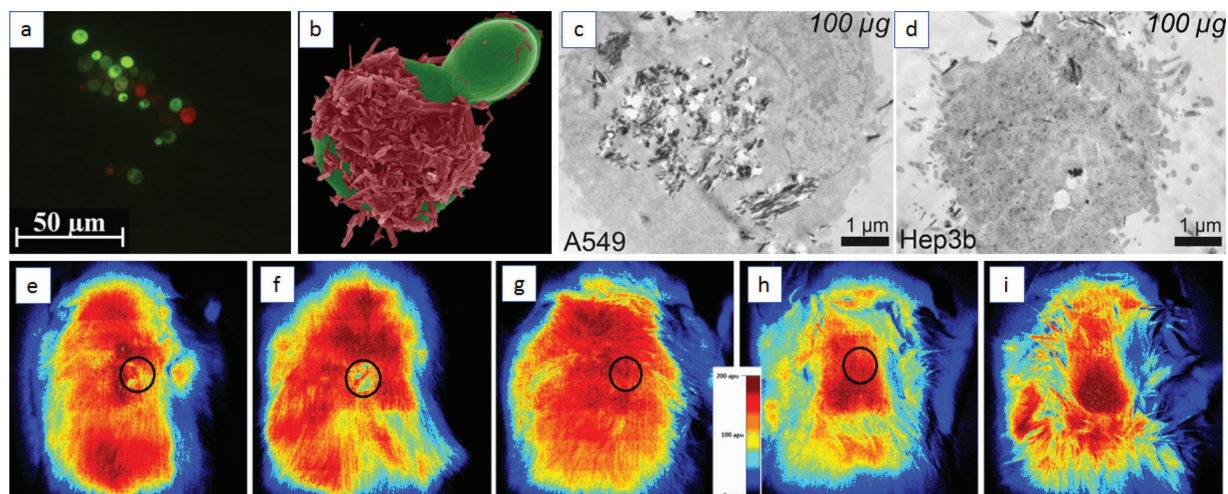


Figure 11. a) Live/dead viability stain of HNTs-coated yeast cells. b) Scanning electron microscopy image of budding HNTs-coated yeast cells.^[52] Transmission electron microscopy images of halloysite uptake by c) A549 and d) Hep3b human cells.^[58] Blood vessels' de novo formation in the implantation area in rats: e) 3 weeks after implantation of chitosan–agarose–gelatin scaffolds, f) 3 weeks after implantation of chitosan–agarose–gelatin scaffolds doped with 6 wt% halloysite, g) 6 weeks after implantation of chitosan–agarose–gelatin scaffolds, h) 6 weeks after implantation of chitosan–agarose–gelatin scaffolds doped 6 wt%, and i) control animal. Black circles indicate the implant area.^[63] Reproduced with permission.^[52,63] Copyright 2013 and 2016, Royal Society of Chemistry. Reproduced under the terms of the Creative Commons Attribution 4.0 International License.^[58] Copyright 2015, Springer Nature.

visible in enhanced dark-field image (Figure 12D, E; micrographs were edited only with linear brightness/contrast adjustment). Colocalization of high-scattering regions in dark-field images and high intensity red channel in fluorescence images confirm the fluorescent properties of the obtained core–shell nanocomposites.

The excitation/emission properties of quantum dots are highly dependent on the particle size. In the obtained composites, the particle size was distributed in 5–10 nm range and corresponds to the broad emission range of HNTs–CdS with blue-region laser excitation. The composites are concentrated at the cells' periphery, and may serve as the complementary staining agent in addition to the nuclei-staining dyes such as DAPI (diamidino-2-phenylindole). The versatile properties of the clay nanotubes (such as presence of outer positively and inner negatively charged surfaces) offer the opportunity to modify the tubule nanocomposites using lumen for the loading of drugs, thus combining diagnostics and therapy (theranostics).

5. Halloysite In Vivo Toxicity

Increasing numbers of biomedical studies and emerging applications of HNTs (currently limited by cosmetics and animal treatment) are in progress. Therefore, their impact on the environment and

human health should be taken into account. In vivo studies employing various organisms also demonstrate high biocompatibility to halloysite. *Caenorhabditis elegans* nematodes were treated with 0.05–1 mg mL⁻¹ nanotubes delivered into the nematode intestines using HNTs-coated bacterial food.^[55]

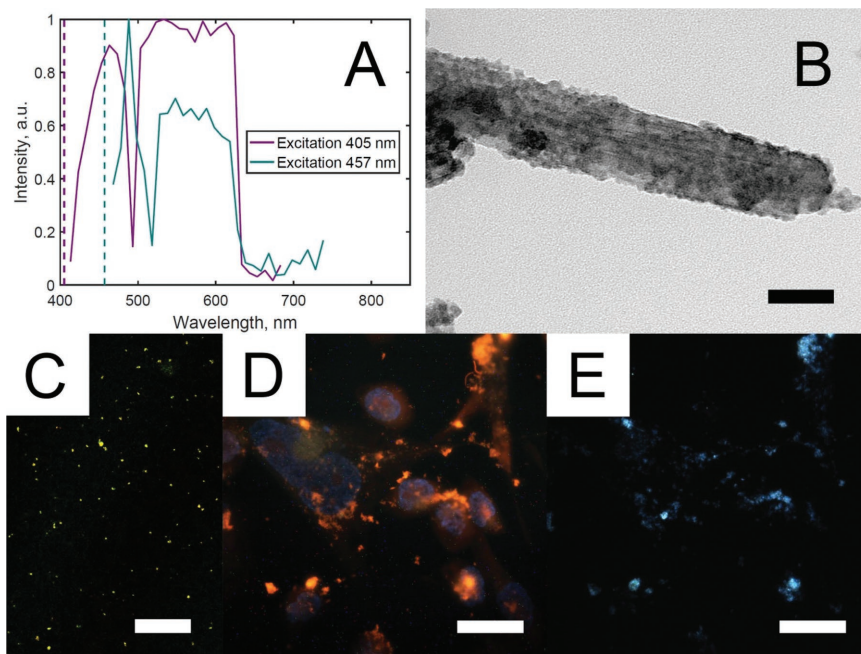


Figure 12. a) Fluorescence spectra of HNTs–CdS composites excited by 405-nm or 457-nm laser, registered with confocal microscope. b) TEM image of the individual HNTs–CdS nanotube. c) Confocal microscopy image of HNTs–CdS composites. PC3 human prostate cancer cells contrasted with HNTs–CdS composites: d) PI and HNTs–CdS fluorescence; e) enhanced dark field. Scale bars: 50 nm (b), 200 μm (c), 20 μm (d), 20 μm (e).

Halloysite within these concentrations was considered to be safe, not damaging the organism of the nematodes. It is likely that halloysite could inflict only mechanical stress onto the nematode's alimentary system; chemotaxis assay has suggested that the microworms intentionally try to avoid the nanotubes. The other *in vivo* study, performed with *Paramecium caudatum* protozoans, has confirmed that halloysite was the most biocompatible as compared with other nanoclays (montmorillonite, bentonite, kaolin) and especially with relatively toxic graphene oxide.^[61] The safe concentration of halloysite for *P. caudatum* was 10 mg mL⁻¹, which is tenfold higher than the concentrations thought to be safe for cell cultures (≈ 0.5 mg mL⁻¹). The confocal microscopy image clearly show that the rhodamine-labeled halloysite was located inside the intestine of the *C. elegans* nematode, **Figure 13a**. However, *in vivo* studies on mice^[62] have shown that at high concentrations (exceeding 50 mg kg⁻¹) orally administered halloysite induces oxidative damage in the liver, likely due to Al³⁺ accumulation. The mice treated with low clay nanotube doses (below 5 mg per kg body weight) have shown no sign of oxidative stress or other toxicity issues. Moreover, the mice administered low doses of halloysite with food demonstrated higher growth rates. The other report demonstrates the good internalization and subsequent blood vessel formation within the implantation site of composite polymer-HNTs tissue engineering scaffolds in rats (**Figure 11e–i**).^[63]

Recently, the cell uptake of halloysite labeled with fluorescein isothiocyanate (FITC-HNTs) and its biodistribution in zebrafish were studied.^[64] The cytotoxicity assays showed that the cell viabilities of human umbilical vein endothelial cells and human breast adenocarcinoma (MCF-7) cells were above 60% after being treated with different nanoclay concentrations (2.5–200 μ g mL⁻¹) for 72 h. The uptake of halloysite by endothelial cells and MCF-7 cells was confirmed via confocal laser scanning microscopy observation. The *in vivo* toxicity of halloysite was then examined in the early development of zebrafish embryos. The percent survival of zebrafish embryos and larvae showed no significant changes at different developmental stages (24, 48, 72, 96, and 120 hpf) when treated with various concentrations of the nanotubes (0.25–10 mg mL⁻¹). Furthermore, halloysite could promote the hatchability of zebrafish embryos and

did not affect the morphological development of zebrafish at a concentration of ≤ 25 mg mL⁻¹. Halloysite was also ingested by zebrafish larvae and accumulated predominantly in the gastrointestinal tract (**Figure 13b**). The fluorescence intensity of FITC-HNTs decreased gradually with time, which suggested that clay nanotubes could be excreted by zebrafish larvae through the gastrointestinal metabolism. It can be concluded that halloysite is a biocompatible and biosafe nanomaterial. The potential inhalation exposure to halloysite was investigated in an industrial research laboratory and no significant exposure risk was found; but cautions should be taken.^[65] Future studies are required to fully investigate the toxic effects of clay nanotubes on human organisms; however, this material is much safer than many other types of clay, graphene, carbon nanotubes, and other nanomaterials.

6. Conclusion and Prospects

Natural HNTs have a high aspect ratio, good adsorption ability, and biocompatibility (low toxicity), which promise a great potential in biomedical areas. The applications of halloysite include sustained drug delivery, tissue scaffold engineering, wound healing dressing, cell capture substrates, biosensors, cell labeling, and bacterial proliferation substrates. These clay nanotubes show 10–20 wt% drug loading ability (with internal/external selectivity driven by the opposite inside/outside surface charges) and can extend the drug delivery time to tens of hours. Halloysite addition can improve the mechanical properties of bio-nanocomposites and cell adhesion on the scaffolds. A drug-loaded halloysite can be doped into the polymer scaffolds for days and weeks of lasting controlled release. These clay nanotubes have strong adsorption ability toward blood and tissue exudates when they are used in wound healing composite materials. The rough surfaces fabricated by self-assembly of HNTs enhance the interactions with tumor cells, and the cell capture efficacy was largely improved.

Since this nanoclay has no toxicity toward bacteria, halloysite can be used in oil/water emulsification for petroleum spill bioremediation. Coating of cells by the nanotube layer can control their growth not harming the viability. CdS quantum dots immobilized on halloysite produces core-shell tubule systems which were successfully used for cell imaging and labeling.

For all bio-applications, the safety of halloysite must be thoroughly controlled. The toxicity of halloysite arises with the needle-like morphology, impurities, and high particle concentration. However, the length of clay nanotubes can be tailored by ultrasonic scission accomplished with uniform viscosity centrifugation and resulted in shorter 0.4–0.5 μ m nanotubes show lower toxicity. The impurities in halloysite can be removed by aqueous washing/centrifugation and aluminum content may be diminished by acid etching; this high-purity nanoclay can be

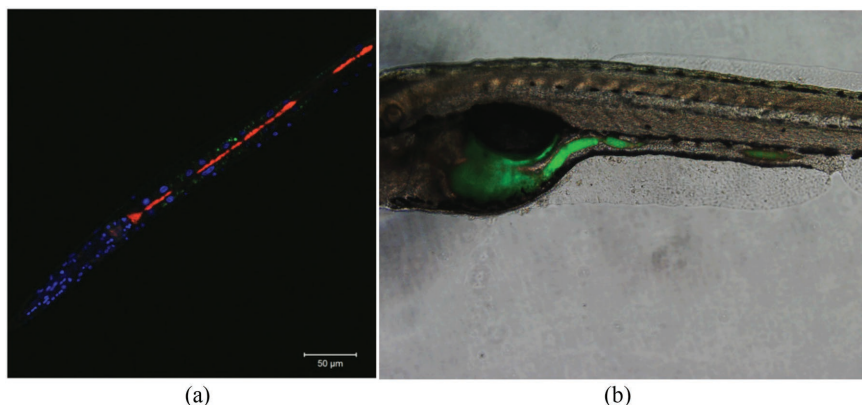


Figure 13. a) Confocal microscopy image of rhodamine-labeled halloysite localization inside the intestines of *Caenorhabditis elegans* nematode.^[55] b) Fluorescence images of zebrafish showing the presence of FITC-labeled halloysite inside the gastrointestinal tract of zebrafish.^[64] Reproduced with permission.^[55,64] Copyright 2015 and 2018, Royal Society of Chemistry.

safely utilized for medicine. Generally, halloysite clay is highly biocompatible and of low toxicity. However, halloysite is not biodegradable in vivo (it may be accumulated harming lung and kidney) and has to be used preferably externally or at very low concentrations if used internally (e.g., for DNA delivery). Though HNTs were successfully utilized for the treatment of animals (piglets, chicken, dogs), their use in human medicine needs further studies.

Acknowledgements

M.L. thanks the support from China Scholarship Council Fund (201706785003), National Natural Science Foundation of China (51473069 and 51502113), and the Pearl River S&T Nova Program of Guangzhou (201610010026). Y.L. and A.N. thank the support from the Ministry of Education and Science of the Russian Federation (Grant No. 14.Z50.31.0035). The part of work performed by R.F. was supported by the Russian Government Program of Competitive Growth of Kazan Federal University and by the subsidy allocated to Kazan Federal University. The authors thank Anna Stavitskaya for providing HNT-CdS composites.

Conflict of Interest

The authors declare no conflict of interest.

Keywords

drug delivery, halloysite nanotubes, self-assembly, toxicity

Received: October 30, 2018

Revised: December 3, 2018

Published online: December 19, 2018

- [1] Y. Lvov, W. Wang, L. Zhang, R. Fakhruddin, *Adv. Mater.* **2016**, *28*, 1227.
- [2] Y. M. Lvov, D. G. Shchukin, H. Mohwald, R. R. Price, *ACS Nano* **2008**, *2*, 814.
- [3] Y. Lvov, E. Abdullayev, *Prog. Polym. Sci.* **2013**, *38*, 1690.
- [4] M. Liu, Z. Jia, D. Jia, C. Zhou, *Prog. Polym. Sci.* **2014**, *39*, 1498.
- [5] P. Pasbakhsh, G. J. Churchman, J. L. Keeling, *Appl. Clay Sci.* **2013**, *74*, 47.
- [6] P. Yuan, D. Tan, F. Annabi-Bergaya, *Appl. Clay Sci.* **2015**, *112–113*, 75.
- [7] M. Massaro, G. Cavallaro, C. G. Colletti, G. Lazzara, S. Milioto, R. Noto, S. Riel, *J. Mater. Chem. B* **2018**, *6*, 3415.
- [8] V. Vergaro, Y. M. Lvov, S. Leporatti, *Macromol. Biosci.* **2012**, *12*, 1265.
- [9] M. Liu, Y. Shen, P. Ao, L. Dai, Z. Liu, C. Zhou, *RSC Adv.* **2014**, *4*, 23540.
- [10] X. Zhang, R. Guo, J. Xu, Y. Lan, Y. Jiao, C. Zhou, Y. Zhao, *J. Biomater. Appl.* **2015**, *30*, 512.
- [11] S. Kumar-Krishnan, A. Hernandez-Rangel, U. Pal, O. Ceballos-Sanchez, F. Flores-Ruiz, E. Prokhorov, O. A. de Fuentes, R. Esparza, M. Meyyappan, *J. Mater. Chem. B* **2016**, *4*, 2553.
- [12] M. J. Mitchell, C. A. Castellanos, M. R. King, *Biomaterials* **2015**, *56*, 179.
- [13] Z. Shu, Y. Zhang, Q. Yang, H. Yang, *Nanoscale Res. Lett.* **2017**, *12*, 135.
- [14] G. Cavallaro, G. Lazzara, S. Milioto, *J. Phys. Chem. C* **2012**, *116*, 21932.
- [15] M. K. Pickett, A. Panchal, N. Crews, Y. Lvov, in *Abstracts of Papers of the American Chemical Society*, Vol. 255, American Chemical Society, Washington, DC **2018**.
- [16] Y. Zhao, G. Cavallaro, Y. Lvov, *J. Colloid Interface Sci.* **2015**, *440*, 68.
- [17] M. Liu, R. He, J. Yang, W. Zhao, C. Zhou, *ACS Appl. Mater. Interfaces* **2016**, *8*, 7709.
- [18] R. He, M. Liu, Y. Shen, Z. Long, C. Zhou, *J. Mater. Chem. B* **2017**, *5*, 1712.
- [19] M. Liu, Z. Huo, T. Liu, Y. Shen, R. He, C. Zhou, *Langmuir* **2017**, *33*, 3088.
- [20] R. He, M. Liu, Y. Shen, R. Liang, W. Liu, C. Zhou, *Mater. Sci. Eng., C* **2018**, *85*, 170.
- [21] R. von Klitzing, D. Stehl, T. Pogrzeba, R. Schomäcker, R. Minullina, A. Panchal, S. Konnova, R. Fakhruddin, J. Koetz, H. Möhwald, *Adv. Mater. Interfaces* **2017**, *4*, 1600435.
- [22] M. Omarova, L. T. Swientoniewski, I. K. M. Tsengam, A. Panchal, T. Yu, D. A. Blake, Y. M. Lvov, D. Zhang, V. John, *ACS Sustainable Chem. Eng.* **2018**, *6*, 14143.
- [23] O. Owoseni, E. Nyankson, Y. Zhang, D. J. Adams, J. He, L. Spinu, G. L. McPherson, A. Bose, R. B. Gupta, V. T. John, *J. Colloid Interface Sci.* **2016**, *463*, 288.
- [24] Y. Hou, J. Jiang, K. Li, Y. Zhang, J. Liu, *J. Phys. Chem. B* **2014**, *118*, 1962.
- [25] D. Kpogbemabou, G. Lecomte-Nana, A. Aimable, M. Bienia, V. Niknam, C. Carrion, *Colloids Surf. A* **2014**, *463*, 85.
- [26] O. Owoseni, Y. Zhang, Y. Su, J. He, G. L. McPherson, A. Bose, V. T. John, *Langmuir* **2015**, *31*, 13700.
- [27] A. Panchal, L. T. Swientoniewski, M. Omarova, T. Yu, D. Zhang, D. A. Blake, V. John, Y. M. Lvov, *Colloids Surf., B* **2018**, *164*, 27.
- [28] B. Bhushan, *Biophysics of Human Hair: Structural, Nanomechanical, and Nanotribological studies*, Springer Science + Business Media, Berlin, Heidelberg **2010**.
- [29] C. Popescu, H. Höcker, *Chem. Soc. Rev.* **2007**, *36*, 1282.
- [30] A. Panchal, G. Fakhruddin, R. Fakhruddin, Y. Lvov, *Nanoscale* **2018**, *10*, 18205.
- [31] R. A. Lodge, B. Bhushan, *J. Appl. Polym. Sci.* **2006**, *102*, 5255.
- [32] R. R. Price, B. P. Gaber, Y. Lvov, *J. Microencapsulation* **2001**, *18*, 713.
- [33] A. C. Santos, C. Ferreira, F. Veiga, R. Antonio J., A. Panchal, Y. Lvov, A. Agarwa, *Adv. Colloid Interface Sci.* **2018**, *257*, 58.
- [34] W. O. Yah, A. Takahara, Y. M. Lvov, *J. Am. Chem. Soc.* **2012**, *134*, 1853.
- [35] G. Cavallaro, G. Lazzara, S. Milioto, F. Parisi, V. Sanzillo, *ACS Appl. Mater. Interfaces* **2014**, *6*, 606.
- [36] B. Amro, K. James, T. Turner, *J. Soc. Cosmet. Chem.* **1993**, *45*, 159.
- [37] C. Cummings, J. C. Finlay, N. E. MacDonald, *Paediat. Child Health* **2018**, *23*, e18.
- [38] C. G. Burkhart, C. N. Burkhart, *Expert Opin. Drug Saf.* **2006**, *5*, 169.
- [39] F. Abdel-Ghaffar, M. Semmler, K. Al-Rasheid, S. Klimpel, H. Mehlhorn, *Parasitol. Res.* **2010**, *106*, 423.
- [40] Y. M. Lvov, M. M. DeVilliers, R. F. Fakhruddin, *Expert Opin. Drug Deliv.* **2016**, *13*, 977.
- [41] Y. Hu, J. Chen, X. Li, Y. Sun, S. Huang, Y. Li, H. Liu, J. Xu, S. Zhong, *Nanotechnology* **2017**, *28*, 375101.
- [42] Z. Long, J. Zhang, Y. Shen, C. Zhou, M. Liu, *Mater. Sci. Eng., C* **2017**, *81*, 224.
- [43] M. Makaremi, P. Pasbakhsh, G. Cavallaro, G. Lazzara, Y. K. Aw, S. M. Lee, S. Milioto, *ACS Appl. Mater. Interfaces* **2017**, *9*, 17476.
- [44] W. Wei, E. Abdullayev, A. Hollister, D. Mills, Y. M. Lvov, *Macromol. Mater. Eng.* **2012**, *297*, 645.
- [45] J. A. Weisman, U. Jammalamadaka, K. Tappa, D. K. Mills, *Bioengineering* **2017**, *4*, 96.
- [46] W. Y. Zhou, B. Guo, M. Liu, R. Liao, A. B. M. Rabie, D. Jia, *J. Biomed. Mater. Res., Part A* **2010**, *93*, 1574.



- [47] M. Liu, C. Wu, Y. Jiao, S. Xiong, C. Zhou, J. Mater. Chem. B **2013**, 1, 2078.
- [48] R. Qi, R. Guo, M. Shen, X. Cao, L. Zhang, J. Xu, J. Yu, X. Shi, J. Mater. Chem. **2010**, 20, 10622.
- [49] G. Lazzara, S. Riela, R. F. Fakhrullin, Ther. Delivery **2017**, 8, 633.
- [50] F. R. Ahmed, M. H. Shoaib, M. Azhar, S. H. Um, R. I. Yousuf, S. Hashmi, A. Dar, Colloids Surf., B **2015**, 135, 50.
- [51] R. Kamaliev, I. Ishmukhametov, S. Batasheva, E. Rozhina, R. Fakhrullin, Nano-Struct. Nano-Objects **2018**, 15, 54.
- [52] S. A. Konnova, I. R. Sharipova, T. A. Demina, Y. N. Osin, D. R. Yarullina, O. N. Ilinskaya, Y. M. Lvov, R. F. Fakhrullin, Chem. Commun. **2013**, 49, 4208.
- [53] A. A. Taylor, G. M. Aron, G. W. Beall, N. Dharmasiri, Y. Zhang, R. J. C. McLean, Environ. Toxicol. **2014**, 29, 961.
- [54] S. Konnova, Y. Lvov, R. Fakhrullin, Clay Miner. **2016**, 51, 429.
- [55] G. I. Fakhrullina, F. S. Akhatova, Y. M. Lvov, R. F. Fakhrullin, Environ. Sci.: Nano **2015**, 2, 54.
- [56] V. Vergaro, E. Abdullayev, Y. M. Lvov, A. Zeitoun, R. Cingolani, R. Rinaldi, S. Leporatti, Biomacromolecules **2010**, 11, 820.
- [57] S. Riela, M. Massaro, C. G. Colletti, A. Bommarito, C. Giordano, S. Milioto, R. Noto, P. Poma, G. Lazzara, Int. J. Pharm. **2014**, 475, 613.
- [58] M. R. Dzamukova, E. A. Naumenko, Y. M. Lvov, R. F. Fakhrullin, Sci. Rep. **2015**, 5, 10560.
- [59] R. Yendluri, Y. Lvov, M. M. de Villiers, V. Vinokurov, E. Naumenko, E. Tarasova, R. Fakhrullin, J. Pharm. Sci. **2017**, 106, 3131.
- [60] A. V. Stavitskaya, A. A. Novikov, M. S. Kotelev, D. S. Kopitsyn, E. V. Rozhina, I. R. Ishmukhametov, R. F. Fakhrullin, E. V. Ivanov, Y. M. Lvov, V. A. Vinokurov, Nanomaterials **2018**, 8, 391.
- [61] M. Kryuchkova, A. Danilushkina, Y. Lvov, R. Fakhrullin, Environ. Sci.: Nano **2016**, 3, 442.
- [62] X. Wang, J. Gong, Z. Gui, T. Hu, X. Xu, Environ. Toxicol. **2018**, 33, 623.
- [63] E. A. Naumenko, I. D. Guryanov, R. Yendluri, Y. M. Lvov, R. F. Fakhrullin, Nanoscale **2016**, 8, 7257.
- [64] Z. Long, Y.-P. Wu, H.-Y. Gao, J. Zhang, X. Ou, R.-R. He, M. Liu, J. Mater. Chem. B **2018**, 6, 7204.
- [65] A. Koivisto, A. Bluhme, K. Kling, A. Fonseca, E. Redant, F. Andrad, NanoImpact, **2018**, 10, 153.